JOURNAL OF PROPULSION AND POWER
Vol. 18, No. 4, July–August 2002

New Fossil Power Systems and the Role of Open-Cycle Magnetohydrodynamics Generators

Naoyuki Kayukawa*
Hokkaido University, Sapporo 060-8628, Japan

Two scenarios for achieving CO_2-free fossil fuel utilization in electric power systems are proposed, and the role of the open-cycle magnetohydrodynamics (MHD) power generation is discussed, taking into account the current trends of power generation systems and fossil fuel utilization. It is emphasized that the oxygen combustion of synthetic fuels, synthesis of primary fuels with exhaust gases and heat with additional steam, and separation of carbon dioxide from a syngas mixture should be performed in the central power stations to provide concentrated CO_2 recovery and hydrogen supply capability for dispersed-type power units. It is shown that MHD power generation driven by plasmas from oxygen-fired synthetic fuel might be the only possible candidate for a topping system in the ultimate base-load power station with the highest efficiency. Four models of central power generation systems were considered on the basis of the presumably attainable performance of the components, and the effects of the proposed scenarios were evaluated in terms of power generation efficiencies with the assumed fractional dependence on the dispersed-type power systems.

Nomenclature

h	=	enthalpy, kJ/kmol
N	=	molar number, kmol
Q	=	heat, kJ
W	=	work, work consumption, kJ
w	=	molar work consumption, kJ/kmol
x	=	C mole number in combustion reaction, Eq. (4)
y	=	C mole number in gasification reaction, Eq. (1)
γ	=	ratio of specific heats
ΔH^0_{fs}	=	standard formation enthalpy of species s, kJ/kmol
δ	=	fraction of hydrogen distributed to topping unit
ε	=	fractional power from dispersed system
η	=	efficiency, %

Subscripts

a	=	absorption
CB, cb	=	combustor, combustion
CP, cp	=	compressor, compression
CS	=	centralized system
D	=	dispersed system
FC	=	fuel compressor
GF	=	gasifier
GT	=	gas turbine
HX	=	radiation-type heat exchanger
LOX	=	liquid oxygen
M	=	magnetohydrodynamic generator
P	=	pump
ph	=	preheat
RFP	=	recuperative fuel preheater
SG	=	steam generator
SGS	=	syngas separator
ST	=	steam turbine
s	=	steam
w	=	water
$w, 0$	=	water at 298 K and 0.1 MPa
(1)	=	inlet
(2)	=	exit

Received 4 June 2001; revision received 8 January 2002; accepted for publication 25 February 2002.

*Professor, Center for Advanced Research of Energy Technology, Kita-ku, Kita 13, Nishi 8; kayukawa@qe.eng.hokudai.ac.jp. Member AIAA.

I. Introduction

THE present trend in electric power generation systems to meet the increased demand for electric power is achieved by small-scale dispersed-type power units driven by renewable energy or hydrogen-rich fossil fuels. This trend has arisen due to global environmental warming, the technological limit of significant improvement in thermal efficiency by increasing the scale and working temperature, and the low load-matching capability of large-scale power stations. This trend and the structure of present power systems are represented in Fig. 1. The environmental impact may largely be reduced by the present dual systems with developments in unit performances and with an increase in the number of on-site facilities. However, the CO_2 emission could not be reduced below some level because of the technological difficulty in gas separation of air combustion products in a central power station and of the use of carbonaceous fuels in a dispersed system. It is also clear that there is a limit of dependence on dispersed-type power sources because of the low-energy density of natural resources and the cost performance of intrinsically small-scale units, such as fuel cells and micro gas turbines. Therefore, a large part of the power demand must be met in the long term by centralized base-load-type power systems. The present world average percentage use of fossil resources as primary fuels in electric power generation is about 63% (Ref. 1) and is gradually decreasing. However, the use of fossil resources is expected to increase continuously as developing countries become more developed and with the increase in global population. At present, the main concern with fossil energy utilization is global warming. However, a comprehensive scenario and technology to achieve the ultimate goal of CO_2-free utilization of carbonaceous fuels in power systems have not yet been established.

This paper describes two realistic scenarios for achieving this goal. The basic concept is that carbon dioxide should be managed in a concentrated manner and that dispersed-power units, including vehicles, should be operated on hydrogen fuel. To design such an energy system, the reforming of carbonaceous fuels to hydrogen, or hydrogen and carbon monoxide synthetic fuels, the separation of hydrogen and carbon dioxide, or of hydrogen, carbon monoxide, and carbon dioxide from synthetic gas mixtures, and the supply of hydrogen to distributed units should be performed in centralized systems operated by recycled synthetic fuel combustion with pure oxygen.

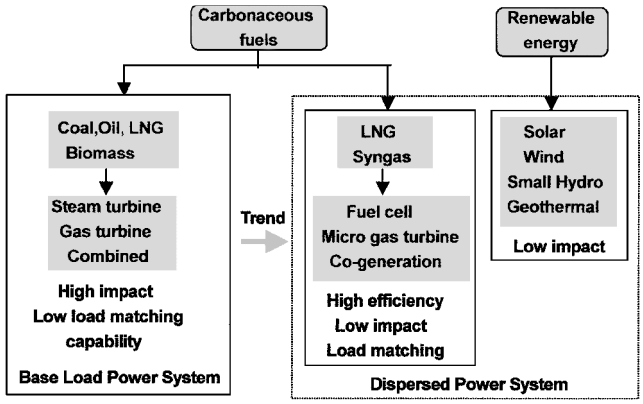

Fig. 1 Trends and features of present electric power generating systems.

II. Basic Concepts

There are two kinds of synthetic reactions for carbonaceous fuel reforming. One is the steam reforming reaction described by

$$C + 2H_2O = 2H_2 + CO_2 + \Delta H^0_{f\,CO_2} - 2\Delta H^0_{f\,H_2O} \qquad (1)$$

where $\Delta H^0_{f\,CO_2} - 2\Delta H^0_{f\,H_2O}$ (=90.18 MJ/kmol C) is the absorbed heat estimated by the standard molar formation enthalpies of CO_2 and H_2O. The reaction proceeds above a temperature of about 870 K. The other reactions are those with carbon dioxide and steam, which are described as

$$C + CO2 = 2CO + 2\Delta H^0_{f\,CO} - 2\Delta H^0_{f\,CO_2} \qquad (2)$$

$$C + H_2O = CO + H_2 + \Delta H^0_{f\,CO} - \Delta H^0_{f\,H_2O} \qquad (3)$$

These reactions proceed at a temperature higher than about 1470 K. According to chemical equilibrium calculations, the volume ratio of hydrogen to carbon monoxide obtained by reactions (2) and (3) is about $\frac{1}{2}$, and the ratio is almost independent of the pressure.[2] Therefore, if 1 kmol C is gasified, $\frac{1}{3}$ kmol C is reformed to $\frac{2}{3}$ kmol CO in reaction (2), and $\frac{2}{3}$ kmol C is synthesized to $\frac{2}{3}$ kmol CO and $\frac{2}{3}$ kmol H_2 in reaction (3). The absorbed heat is 145.1 MJ in total. Hereafter, energy utilization systems based on reaction (1) and those based on reactions (2) and (3) are named scenario 1 and scenario 2, respectively.

In the conventional process of carbonaceous fuel reforming, reaction heat is provided by partial combustion of the fuel itself. In this case, the maximum obtainable combustion heat of the synthetic fuel is equal to the heat obtained by direct combustion of the primary fuel. In the case of reaction (1), this can be shown as follows: We assume that total consumption of C in the combustion reaction

$$C + O_2 = CO_2 + \Delta H^0_{f\,CO_2} \qquad (4)$$

and in the gasification reaction (1) is given by $x + y = 1$. The gasification heat is $y(\Delta H^0_{f\,CO_2} - 2\Delta H^0_{f\,H_2O})$, and it should be equal to the combustion heat given by $-x\Delta H^0_{f\,CO_2}$. Then, we obtain $y = \Delta H^0_{f\,CO_2}/2\Delta H^0_{f\,H_2O}$ kmol. The H_2 mole number obtained from the reaction (1) is $2y$, of which combustion heat is $-2y\Delta H^0_{f\,H_2O} = -\Delta H^0_{f\,CO_2}$, that is, the combustion heat of 1 kmol C. If the same calculations are applied to reactions (2) and (3), the synthetic fuel mole numbers are approximately 0.9743 and 0.4871 kmol for CO and H_2, respectively. Again, the total combustion heat of CO and H_2 is equal to that of 1 kmol C.

The preceding calculations show that the reforming heat absorbed as chemical energy of the synthetic fuel is delivered as thermal energy through the combustion reaction. Therefore, if the reforming heat could be supplied from exhaust gases of an appropriate high-temperature unit, and the unit could be driven by synthetic fuel that has been recycled, the combustion heat released in the unit would be higher than the combustion heat of the primary fuel by the amount of the absorbed heat. In other words, the amount of primary fuel input to the gasifier could be decreased by an amount corresponding to the absorbed heat. The concept of this thermochemical pumping is one of the bases for designing efficient CO_2-free energy systems. Because of the higher reaction heat in reactions (2) and (3) than that in reaction (1), the effect of thermochemical pumping is much higher in principle in scenario 2 than in scenario 1.

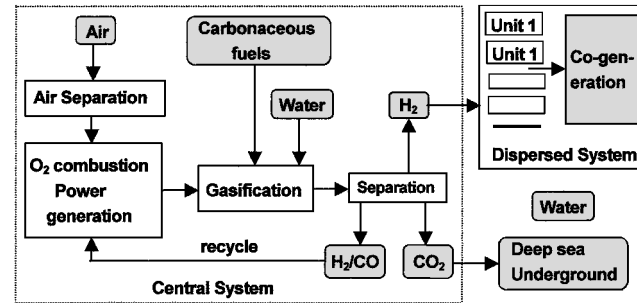

Fig. 2 Concept of thermochemical pumping for CO_2-free fossil fuel power generation systems.

Note that the combustion of recycled hydrogen or a hydrogen/carbon monoxide mixture in the topping unit should be performed with pure oxygen for the following reasons: 1) Pure H_2O and/or H_2O and CO_2 are supplied to the gasifier incorporated downstream of the topping unit. 2) There is minimum NO_x emission. 3) It allows for easy syngas separation downstream of the system. The proposed concept is illustrated in Fig. 2. The recycled fuels are hydrogen in scenario 1 and a mixture of hydrogen and carbon monoxide in scenario 2. The processes enclosed by broken lines should be performed in the centralized power station. In both cases, an appropriate amount of hydrogen should be supplied to distributed power units, including vehicles. In these scenarios, the carbon dioxide can be managed in a concentrated manner, and the heat regeneration is performed basically through gasification processes. Some of the separated CO_2 could be fed to biomass plants of the microalgae types,[3] where chlorella (i.e., the food and the oxygen production) could be carried out photosynthetically. The remainder of the CO_2 is liquefied, and some of this liquefied CO_2 could be used commercially and the rest stored in deep sea or underground. On the other hand, cogenerative heat use may be the most efficient method for utilization of energy in dispersed power units in regard to the amount of each exhaust heat and the diffusive nature of the heat.

When the level of temperature and heat to be absorbed in the reforming processes is taken into account, a topping power generation unit for scenario 1 should be either a high-temperature gas turbine with steam or water injection to meet the allowable turbine inlet temperature or an open-cycle magnetohydrodynamics (MHD) generator in which an appropriate amount of steam should be injected downstream of the MHD generator to provide reforming steam. On the other hand, in scenario 2, the gasification reaction temperature should be higher than 1470 K, so that if we assume there is a topping unit with ~35% thermal efficiency, the required working temperature is as high as 2300 K, a temperature to which no rotational power generation units could be adapted. Therefore, an open-cycle MHD generator might be the only appropriate topping unit in systems of scenario 2. A temperature of about 3300 K, which might be attainable with preheated CO and H_2 mixture combustion with pure oxygen, may also be suitable for an efficient MHD power generation because of high electrical conductivities. The alkaline seed in the MHD working gas may also promote the gasification process catalytically. Also, in the case of coal gasification with MHD exhausts, desulfurization in the form of solid K_2SO_4 can also be attained[4] at downstream components at a temperature below 1100 K, that is, at a radiant-type heat exchanger and filters or electric precipitators. The concept of a chemical regeneration MHD cycle has also been studied analytically and experimentally by Gannon et al.[5] Major topics and new schema considered in this paper are the following: the separation of syngas and CO_2, a thorough heat recovery by syngas preheating and steam generation, the effects of chemical pumping, the oxygen combustion in MHD combustors, and the effect of hydrogen-fueled dispersed systems on the total efficiency.

III. Model Systems

We consider a hydrogen/oxygen-fired gas turbine and an MHD generator driven by preheated hydrogen/carbon monoxide/oxygen combustion plasmas as topping units for the model systems of scenarios 1 and 2, respectively. The bottoming system is a steam turbine of an existing model[6] in both scenarios, with steam temperature of 840 K, pressure of 25 MPa, and thermal efficiency of $\eta_S \approx 48.5\%$, where η_S is the ratio of generator output and input heat to the steam turbine. The primary fuel is assumed to be coal.

As models for scenario 1, and for the purpose of comparison, we consider two systems. In system 2, shown in Fig. 3, the gasification heat is provided by partial combustion of the primary fuel. The gasifier is installed upstream of the gas turbine (GT) as in the so-called integrated gasification combined cycle (IGCC) system. This is a reference system to system 2 shown in Fig. 4, where the gasifier (GF) is placed downstream of the GT driven by recycled hydrogen. Because the GF temperature in systems 1 and 2 is relatively low ($\sim$1000 K), we assume that coal ash can be extracted in a solid state at the GF. In both systems, the GT fuel is not preheated, and an appropriate amount of steam or water should be injected into the GT combustors to decrease the combustion product temperature to an allowable turbine inlet temperature. Referred to an existing GT,[7] the inlet temperature and the pressure ratio are assumed to be 1770 K and 20, respectively. In system 1, the GT exhaust heat is recovered at the secondary steam generator (SG2) by steam generation for both the steam turbine and the injection into the GT combustor, whereas in system 2, the heat is primarily recovered by coal gasification and secondarily by steam generation. The GT exhaust pressure in system 1 is equal to the SG2 inlet pressure, which is assumed to be 0.15 MPa, and that in system 2 is equal to the GF pressure, which is assumed to be 0.2 MPa. The turbine inlet pressure is determined by the pressure ratio with each exit pressure given earlier. The fuel compressor work is estimated by assuming an adiabatic compression. Although the work is less in an isothermal compression than in an adiabatic counterpart, the total efficiency is higher in the latter case than in the former case because the compressor work can be added to the heat released in the combustor. The oxidant for the GT combustor and for the GF in system 1 is assumed to be supplied from a liquid oxygen storage. The conventional method for liquefaction is assumed in air separation, and the work consumption is estimated by oxygen molar consumption multiplied by the enthalpy difference between the standard state (298 K, 0.1 MPa) and the liquid O_2 storage state. The heat for O_2 vaporization and preheat up to 298 K is assumed to be given at the condenser of the steam cycle. The oxidant supply to each unit is assumed to be provided by the O_2 storage pressure. The GF exit temperatures in system 1 are determined by adjusting the injected steam temperature to be higher than the assumed minimum value of 950 K, whereas those in system 2 are assumed to be higher than the steam temperature for the steam turbine by 50 K. Injection of steam into the GF is not necessary in system 2, because the steam injected into the GT combustor is sufficient for the reforming of carbon to hydrogen even when half of the synthetic hydrogen is distributed to the dispersed system. The gas separation work at the syngas separator (SGS) is assumed to be equivalent to the isothermal compression work for the pressure ratio of 5 in all systems discussed in this paper.

As models for scenario 2, we can also consider two systems according to the design of the fuel preheater, namely, a radiation-type preheater (HX/SG2) operated at temperatures below 1100 K and a recuperative-type fuel preheater (RFP) installed next to the GF and operated at temperatures below 1700 K. The former and the latter systems are shown in Figs. 5 and 6, respectively. In these cases, the topping units are MHD generators that are driven by alkaline-seeded combustion plasmas of preheated hydrogen/carbon monoxide mixture burnt with pure oxygen. Compared with the temperature 2920 K of the U-500 natural gas combustion plasma with preheated air at about 1920 K (Ref. 8), the temperature and the electrical conductivity are sufficiently high in the present case, namely, higher than 3300 K and 26.5 S/m. The plasma interaction with the magnetic field is much higher than that of the U-500. Therefore, we can assume the MHD unit efficiency of 30% in both systems considering the U-500

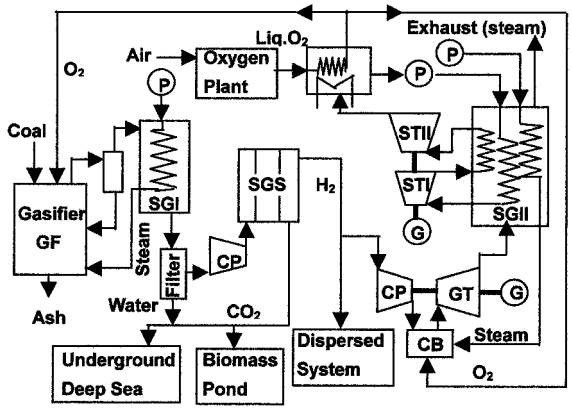

Fig. 3 System 1 of scenario 1 with conventional gasification schematics: CB, combustor; G, turbogenerator; and P, pump.

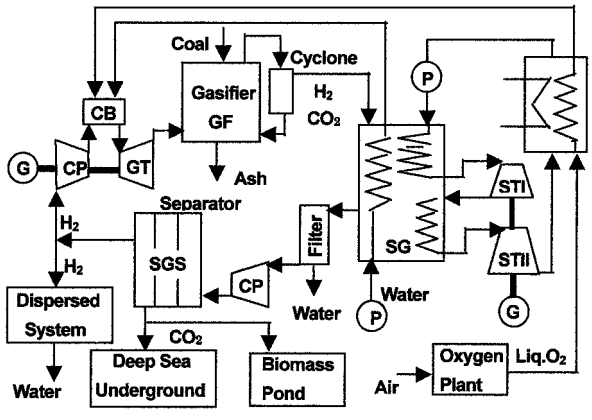

Fig. 4 System 2 of scenario 1 with the combination of GT and GF based on the thermochemical pumping concept.

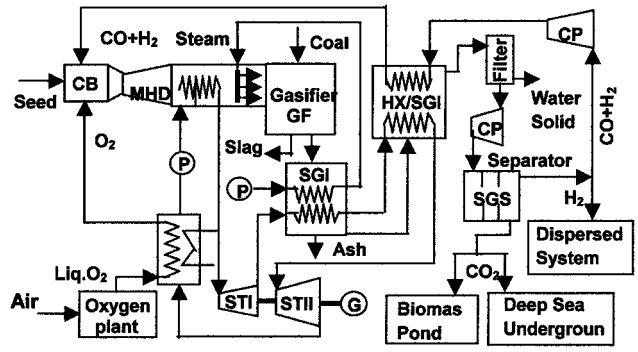

Fig. 5 System 3 of scenario 2 with MHD topping and ST bottoming with a radiant-type heat exchanger.

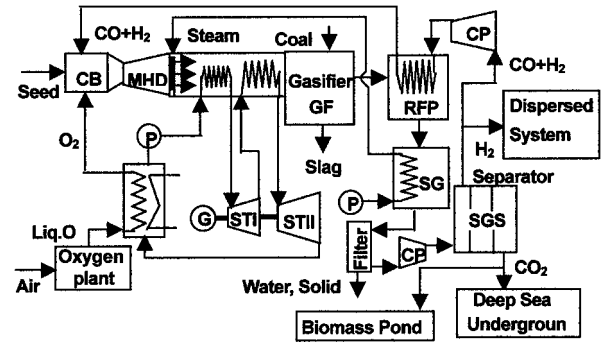

Fig. 6 System 4 of scenario 2 with a RFP.

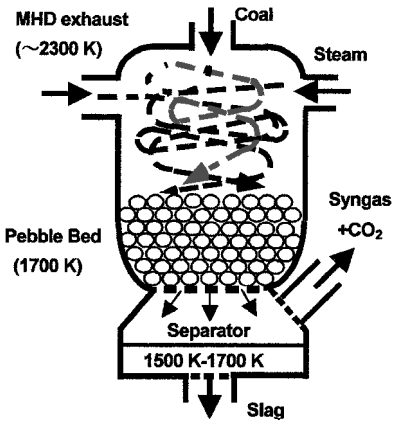

Fig. 7 Design concept of a pebble-bed-type gasifier and coal slag separator.

design value of 24.7%. The generator size may be the same scale, that is, 17 m, as the reference channel with higher power output. In these MHD topping systems 3 and 4, the exhaust gas temperature is higher than 2300 K, below which the electrical conductivity becomes effectively zero, so that the coal ash is in the liquid and/or vapor phase in the GF. To extract the slag in the liquid phase at the GF, we assume that the GF exit temperature is 1700 K. As for the GF design, we can consider a pebble bed type,[9] as shown in Fig. 7, in which the slag can forcibly be injected into the slag separator. The pebble bed design may also provide a sufficiently long reaction time even in a compact reactor. The ceramic pebble balls should be coated with metal that is not eroded with both the coal slag and the alkaline seed in the MHD working gas. There are several advantages in the syngas/oxygen combustion MHD cycle with the thermochemical coal conversion over the direct coal-fired MHD counterpart. One is the exclusion of a high-temperature recuperative air heater that cannot be incorporated in the direct coal-fired MHD system due to slag condensation in the air inlet part at low temperatures. Particular technological difficulties such as an enhanced anode oxidation and the cathode Hall-shorting due to ionic current transport through the slag layers can also be overcome. The second advantage is the heat pumping effect mentioned in Sec. II. In principle, the channel heat input is higher by the gasification heat than that of the direct combustion of coal of the same amount. The volume of the syngas/oxygen combustion product is much less than that of the coal/air combustion. This effect also increases the plasma temperature and the electrical conductivity.

To maintain the exit syngas temperature at the preceding value, and to perform the gasification of a constant amount of coal with MHD exhaust gases with different H_2O fractions, an appropriate amount of heat should be extracted by steam generation for the bottoming system and also an appropriate amount of steam should be injected into the GF. In the system shown in Fig. 5, the syngas heat corresponding to the temperature drop from 1700 to 1100 K is extracted at the primary steam generator (SG1), and the heat below 1100 K is further recovered by steam generation and fuel preheating at the secondary regenerator (HX/SG2), where the fuel preheating temperature is assumed to be 1060 K. The syngas separation from CO_2 is performed at the SGS with the same work consumption as in the two systems of scenario 1. After gas separation, a fraction of hydrogen is distributed to the dispersed power system, and the remaining syngas fuel (H_2 and CO) is returned to the MHD combustor through the fuel compressor and the preheater. Adiabatic compression processes up to 0.77 MPa in system 3 and 0.8 MPa in system 4 are assumed for the same reason as that in the GT compressors. The MHD combustor pressure is 0.75 MPa in both cases. In system 4 (Fig. 6), the heat of syngas with CO_2 entering RFP can almost be recovered by preheating the fuel recycled to the MHD combustor up to 1660 K. The remaining heat of syngas is recovered by generating steam that is injected into the GF. Steam generation for the Rankine cycle is performed upstream of the GF to maintain the GF exit temperature at 1700 K.

IV. Mass and Energy Balance

To minimize ambiguities in calculations and comparisons, we introduce the following assumptions: 1) The combustion and gasification reactions can be described by overall reactions. 2) The reaction heat can be estimated by the standard formation enthalpies. 3) The gaseous enthalpies are estimated by the database in Ref. 10, and those outside the range of temperatures and pressures are estimated by reference to the JANAF thermochemical tables.[11] 4) All processes are adiabatic, that is, wall heat losses in components and piping are neglected. 5) The fractional power from the hydrogen-driven dispersed units is estimated by the average efficiency of $\eta_D = 40\%$ in all cases. 6) The cogeneration is not considered in the calculation of efficiencies. 7) It is assumed that pure oxygen is used as the combustion oxidant in the GF of system 1 for comparison on a common basis, and the NO_x decomposition heat is not considered in any of the systems. The fuel desulfurization work is also not considered in systems 1 and 2. Heat losses accompanying ash or slag removal are also neglected in all cases.

The total net electrical work of the centralized systems can be written as

$$W_{CS} = \sum_i W_i - \sum_j W_j \tag{5}$$

where the first term represents the electrical work output from the GT ($i = \mathrm{GT}$), steam turbine (ST) ($i = \mathrm{ST}$), and/or the MHD generator ($i = \mathrm{M}$), and the second term represents the work consumption in the liquid O_2 (LOX) production ($j = \mathrm{LOX}$), work for the SGS ($j = \mathrm{SGS}$), the pump work ($j = P_1, P_2, \ldots$), and the fuel compression work in systems 3 and 4 ($j = \mathrm{FC}$). The work at the GT compressor is evaluated as the net turbine efficiency.

The electrical work output in dispersed power units may be estimated from the assumption (5) as

$$W_D = [\varepsilon/(1-\varepsilon)]W_{CS} = \eta_D Q_D \tag{6}$$

where Q_D is the total combustion heat of the hydrogen supplied to the dispersed system. The relationship between the hydrogen mole fraction distributed to the topping unit and the fractional power of the dispersed system is given by

$$\varepsilon = \frac{\eta_D(1-\delta)N_{H_2}\left(-\Delta H^0_{f\,H_2O}\right)}{W_{CS} + \eta_D(1-\delta)N_{H_2}\left(-\Delta H^0_{f\,H_2O}\right)} \tag{7}$$

where N_{H_2} is the total synthesized hydrogen mole number. The total electrical efficiency is estimated by

$$\eta = \frac{W_{CS} + W_D}{N_C\left(-\Delta H^0_{f\,CO_2}\right)} \tag{8}$$

where N_C is the carbon mole number in the primary fuel.

A. System 1

In Sec. II., we showed the maximum hydrogen mole number obtained by conventional gasification of 1-kmol C from an energy balance between the gasification and combustion heat. As for the system, however, the temperature of the reactor must be kept above the required level, and the reforming steam should be generated by the heat of syngas. The mass and heat balance should, therefore, be reestimated. The heat balance at the GF can be written as

$$Q_{cb} + Q_s + Q_{O_2} = Q_a + Q^{(2)}_{GF} \tag{9}$$

Because C mole numbers consumed in reactions (4) and (1) are x and y, respectively, we can write $Q_{cb} = -x\Delta H^0_{f\,CO_2}$, $Q_s = 2yh_s$, $Q_{O_2} = xh_{O_2}$, $Q_a = y(\Delta H^0_{f\,CO_2} - 2\Delta H^0_{f\,H_2O})$, and $Q^{(2)}_{GF} = (x+y)h^{GF(2)}_{CO_2} + 2yh^{GF(2)}_{H_2}$. The heat balance at the steam generator is written as

$$Q^{(1)}_{SG1} + Q_w = Q_s + Q^{(2)}_{SG1} \tag{10}$$

Here, the heat of feed water is given by $Q_w = 2yh_w$. Given $Q^{(2)}_{GF} = Q^{(1)}_{SG1}$, the following equation is obtained from Eqs. (9) and (10):

$$x\left(-\Delta H^0_{f\,CO_2}\right) + xh_{O_2} + 2yh_w = y\left(\Delta H^0_{f\,CO_2} - 2\Delta H^0_{f\,H_2O}\right) + 2yh^{SG1(2)}_{H_2} + (x+y)h^{SG1(2)}_{CO_2} \tag{11}$$

Because $x + y = 1$, we obtain

$$x = \frac{h^{SG1(2)}_{CO_2} + 2h^{SG1(2)}_{H_2} - 2h_w + \Delta H^0_{f\,CO_2} - 2\Delta H^0_{f\,H_2O}}{h_{O_2} + 2h^{SG1(2)}_{H_2} - 2h_w - 2\Delta H^0_{f\,H_2O}}$$

$$y = \frac{h_{O_2} - h^{SG1(2)}_{CO_2} - \Delta H^0_{f\,CO_2}}{h_{O_2} + 2h^{SG1(2)}_{H_2} - 2h_w - 2\Delta H^0_{f\,H_2O}} \tag{12}$$

We assume that the gaseous temperature and pressure at the SG1 exit are 355 K and 0.1 MPa, respectively; the temperature of the feed water and oxygen is 298 K; and the pressures of the water and the oxygen are 1.5 MPa and 0.2 MPa, respectively. Then, estimating the enthalpies as values relative to those at 298 K and 0.1 MPa, we obtain $x = 0.1961$ kmol and $y = 0.8039$ kmol from Eq. (12).

With these molar numbers, and the GF and the steam pressures given earlier, the GF and the steam temperatures are calculated from Eqs. (9) and (10) to be 1256 and 600 K, respectively. The injected steam mole number is given by $2y = 1.6078$ kmol. The oxygen work for the GF is then $W_{LOX} = xw_{LOX} = 1.931 \times 10^3$ kJ. Likewise, because the CO_2 plus H_2 mole number is 2.6078 kmol, the work for CO_2 separation is $W_{SGS} = 12.387 \times 10^3$ kJ.

After the CO_2 separator, a fraction δ of hydrogen is introduced into the GT compressor. The energy balance at the GT combustor is then

$$2y\delta h^{CB(1)}_{H_2} + y\delta h^{CB(1)}_{O_2} + N_w h^{CB(1)}_w + 2y\delta\left(-\Delta H^0_{f\,H_2O}\right) = (2y\delta + N_w)h^{GT(1)}_{H_2O} \tag{13}$$

where $h^{CB(1)}_{H_2}$ is estimated at the compressor exit temperature and pressure. The combustor pressure is 3.0 MPa, corresponding to the GT pressure ratio assumed to be 20 and the turbine exit pressure of 0.15 MPa, which is equal to the SG2 inlet pressure. The combustor inlet temperature is estimated by the adiabatic compression in the compressor with the inlet conditions 355 K and 0.1 MPa. The oxygen enthalpy $h^{CB(1)}_{O_2}$ is estimated at the temperature 298 K and the pressure equal to 3.0 MPa. We assume the saturated water injection, and $h^{CB(1)}_w$ are estimated at 480 K and 3.0 MPa. The enthalpy $h^{GT(1)}_{H_2O}$ of the total H_2O is estimated at the turbine inlet conditions of 1770 K and 3.0 MPa. In the case, for example, where $\delta = 0.85$, the injected water mole number is obtained as $N_w = 2.3467$ kmol from Eq. (13). The FC work W_{cp}, and the net axial work done by the GT are, respectively, given by

$$W_{cp} = 2y\delta\left(h^{CP(2)}_{H_2} - h^{CP(1)}_{H_2}\right) \tag{14}$$

$$W_{GT} = \eta_{GT}(2y\delta + N_w)h^{GT(1)}_{H_2O} \tag{15}$$

System 1 is a reference for system 2 described in the next section for the evaluation of the effect of thermochemical pumping. In this respect, we assume the same turbine efficiency η_{GT} as a function of δ shown in Fig. 8. The calculation of η_{GT} will be shown in the next section. The heat balance at the SG2 can be written as

$$(2y\delta + N_w)h^{GT(1)}_{H_2O}(1 - \eta_{GT}) - W_{cp} = Q_{ST} + (2y\delta + N_w)h^{SG2(2)}_{H_2O} + N_w\left(h^{CB(1)}_w - h^{CB(1)}_{w,0}\right) \tag{16}$$

where the enthalpy of supply water for the GT injection is estimated at 298 K and 3.0 MPa. For the case where $\delta = 0.85$, the GT work is 103.23×10^3 kJ and the net axial turbine efficiency is 26.53%. The gas temperature at the turbine exit can be estimated from the left-hand side of Eq. (16) for H_2O mole numbers $N_{H_2O} = 2y\delta + N_w$ as shown in Fig. 8. It can be seen that the temperatures are sufficiently high for steam generation at the assumed temperature. The heat input to the ST system is given by $Q_{ST} = N^{ST}_w(h^{ST(1)}_s - h^{P(2)}_{w,0})$. With an assumed efficiency of 48.5%, the ST output is 102.84×10^3 kJ. The estimated work of the dispersed system is 29.03×10^3 kJ. The steam molar flow in the ST cycle is estimated to be 3.60 kmol, and the pump work is 1.43×10^3 kJ. The pump work for the GT and that for the GF injection are 0.12×10^3 and 39 kJ, respectively. Then, from Eq. (8), the total electrical efficiency of the system 1 is estimated to be 53.9%. The fractional power from the dispersed systems is $\varepsilon = 13.68\%$ in the case of $1 - \delta = 0.15$.

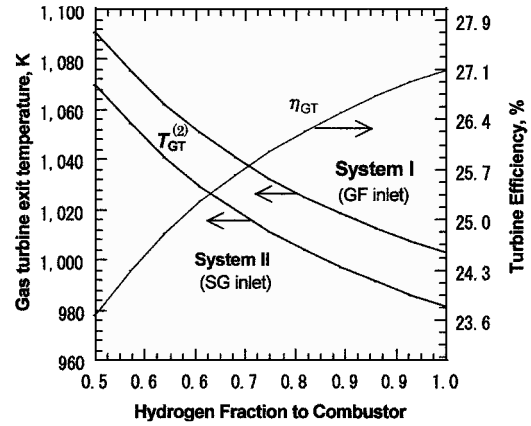

Fig. 8 GT efficiency and exit temperatures in systems 1 and 2.

B. System 2

In system 2, carbon can be reformed as described by reaction (1) with high-temperature exhaust from the GT. For the same turbine pressure ratio of 20 and GF pressure of 0.2 MPa as in system 1, the turbine inlet pressure is calculated to be 4.0 MPa. It is assumed that the combustor pressure and the compressor exit pressure are equal to 4.0 MPa. The fuel temperature at the combustor inlet is calculated by assuming an adiabatic compression from 355 K and 0.1 MPa to 4.0 MPa. Then, with the condition $y = 1$, the heat input and the amount of the injected water to the combustor can be estimated by Eq. (13), where $h^{CB(1)}_w$ should be estimated at 4.0 MPa. The compressor work can be calculated by Eq. (14). Note that, in this case, the molar number of the injected water plus combustion product is sufficient for the reforming, so that no steam is supplied to the GF from the steam generator, and as 2 kmol H_2O is consumed in the gasification reaction, the energy balance at the GF can be written as

$$(2\delta + N_w)h^{GT(1)}_{H_2O}(1 - \eta_{GT}) - W_{cp} = \Delta H^0_{f\,CO_2} - 2\Delta H^0_{f\,H_2O} + (2\delta + N_w - 2)h^{GF(2)}_{H_2O} + h^{GF(2)}_{CO_2} + 2h^{GF(2)}_{H_2} \tag{17}$$

The right-hand side is the reforming heat plus the heat at the GF exit, which are assumed to be equal to the heat input to the steam generator (SG). The molar enthalpies are estimated with the assumed SG pressure of 0.15 MPa and the temperature being higher than the steam temperature by 50 K. With these assumptions, we can calculate the GT exit temperature and enthalpy $h^{GT(2)}_{H_2O}$ for the H_2O mole number equal to $2\delta + N_w$. We can then estimate the GT work and the net axial efficiency as

$$W_{GT} = (2\delta + N_w)\left(h^{GT(1)}_{H_2O} - h^{GT(2)}_{H_2O}\right) - W_{cp} \tag{18}$$

$$\eta_{GT} = \frac{W_{GT}}{(2\delta + N_w)h^{GT(1)}_{H_2O}} \tag{19}$$

The calculated turbine exit temperatures and efficiencies are given in Fig. 8. As mentioned in the preceding section, these efficiencies were employed for the performance evaluation of system 1. The difference between the turbine exit temperatures in the two systems is mainly attributed to the difference in pressures at the GF in system 1 and at the SG in system 2.

The heat balance at the SG is

$$(2\delta + N_w - 2)h^{\mathrm{SG}(1)}_{\mathrm{H_2O}} + h^{\mathrm{SG}(1)}_{\mathrm{CO_2}} + 2h^{\mathrm{SG}(1)}_{\mathrm{H_2}} = Q_{\mathrm{ST}} + N_w\left(h^{\mathrm{CB}(1)}_{w} - h^{\mathrm{CB}(1)}_{w,0}\right) + (2\delta + N_w - 2)h^{\mathrm{SG}(2)}_{\mathrm{H_2O}} + h^{\mathrm{SG}(2)}_{\mathrm{CO_2}} + 2h^{\mathrm{SG}(2)}_{\mathrm{H_2}} \quad (20)$$

The work consumption at the separator and that of the LOX for the GT combustor are, respectively, calculated as $W_{\mathrm{SGS}} = 3w_{\mathrm{SGS}}$ and $W_{\mathrm{LOX}} = \delta w_{\mathrm{LOX}}$, where the molar work consumptions are $w_{\mathrm{SGS}} = 4.75 \times 10^3$ kJ/kmol for the pressure ratio of 5 at 355 K and $w_{\mathrm{LOX}} = 9.89 \times 10^3$ kJ/kmol for LOX production at 140 K and 4.0 MPa. In the case of $\delta = 0.85$, the total efficiency is 55.94% and the fractional power from the dispersed system is 13.2%.

C. System 3

As mentioned in Sec. II, the molar ratio of CO to H_2 in the synthesized gas obtained by reactions (2) and (3) is about 2, and, as confirmed in Ref. 2, no significant effect in system performance results from some change in the syngas composition, so that we can assume here that $N_{\mathrm{CO}}/N_{\mathrm{H_2}} = 2$. Then, CO and H_2 mole numbers from gasification of 1-kmol C are $N_{\mathrm{CO}} = \frac{4}{3}$ and $N_{\mathrm{H_2}} = \frac{2}{3}$ kmol, respectively, of which all of the carbon monoxide plus $N_{\mathrm{H_2}}\delta$ kmol hydrogen should be returned to the topping MHD combustor. The CO_2 and H_2O inputs to the GF from the MHD unit are equal to N_{CO} and $N_{\mathrm{H_2}}\delta$ kmol, respectively. Therefore, the minimum injection steam at the MHD diffuser is $N^{\mathrm{GF}}_s = N_{\mathrm{H_2}}(1-\delta)$ kmol. The syngas contains 1 kmol carbon dioxide. In this system, the GF exit temperature should be kept constant below the slag vaporization temperature, so that an appropriate amount of heat Q_{s1} should be extracted by steam generation from the MHD diffuser.

After the GF, the heat of the syngas and the carbon dioxide mixture should be decreased at SG1 down to the temperature of 1100 K through steam generation for coal reforming at 500 K and 0.5 MPa by $Q^{\mathrm{GF}}_s = N^{\mathrm{GF}}_s(h^{\mathrm{GF}}_s - h^{\mathrm{GF}}_{w,0})$ and for the ST at the pressure of 24 MPa by Q_{s2}. The syngas is further cooled in the heat exchanger (HX/SG2) of the piping type through secondary steam generation by Q_{s3} and the preheating of the syngas recycled to the MHD combustor by

$$Q_{\mathrm{ph}} = N_{\mathrm{CO}}\left(h^{\mathrm{HX}(2)}_{\mathrm{CO}} - h^{\mathrm{HX}(1)}_{\mathrm{CO}}\right) + N_{\mathrm{H_2}}\delta\left(h^{\mathrm{HX}(2)}_{\mathrm{H_2}} - h^{\mathrm{HX}(1)}_{\mathrm{H_2}}\right) \quad (21)$$

where the enthalpies at the exit with the superscript HX(2) are estimated at the assumed temperature of 1060 K and the MHD combustor pressure. The enthalpies at the heat exchanger inlet with the superscript HX(1) are estimated by the exit conditions of the fuel compressor at $p^{(2)}_{\mathrm{FC}} = 0.77$ MPa and $T^{(2)}_{\mathrm{FC}} = (p^{(2)}_{\mathrm{FC}}/p^{(1)}_{\mathrm{FC}})^{(\gamma-1)/\gamma}$, and the compressor inlet conditions are assumed to be $T^{(1)}_{\mathrm{FC}} = 355$ K and $p^{(1)}_{\mathrm{FC}} = 0.1$ MPa. The work for FC can be estimated by

$$W_{\mathrm{FC}} = N_{\mathrm{CO}}\left(h^{\mathrm{FC}(2)}_{\mathrm{CO}} - h^{\mathrm{FC}(1)}_{\mathrm{CO}}\right) + N_{\mathrm{H_2}}\delta\left(h^{\mathrm{FC}(2)}_{\mathrm{H_2}} - h^{\mathrm{FC}(1)}_{\mathrm{H_2}}\right) \quad (22)$$

Then, neglecting the effect of the ionization seed, the heat output from the MHD combustor can be estimated as

$$Q_{\mathrm{M}} = N_{\mathrm{CO}}\left(\Delta H^0_{f\,\mathrm{CO}} - \Delta H^0_{f\,\mathrm{CO_2}}\right) + N_{\mathrm{H_2}}\delta\left(-\Delta H^0_{f\,\mathrm{H_2O}}\right) + N_{\mathrm{O_2}}h^{M(1)}_{\mathrm{O_2}} + N_{\mathrm{CO}}h^{\mathrm{HX}(2)}_{\mathrm{CO}} + N_{\mathrm{H_2}}\delta h^{\mathrm{HX}(2)}_{\mathrm{H_2}} \quad (23)$$

Here, $N_{\mathrm{O_2}}$ is equal to $(N_{\mathrm{CO}} + N_{\mathrm{H_2}})/2$. The oxygen enthalpy is estimated at 298 K and a combustor pressure of 0.75 MPa. The MHD generator work can be estimated by $W_{\mathrm{M}} = \eta_{\mathrm{M}} Q_{\mathrm{M}}$. The LOX work is given by $W_{\mathrm{LOX}} = N_{\mathrm{O_2}} w_{\mathrm{LOX}}$.

The heat input to the gasifier can be written as

$$Q^{(1)}_{\mathrm{GF}} = Q_{\mathrm{M}}(1-\eta_{\mathrm{M}}) + N_{\mathrm{H_2}}(1-\delta)h^{\mathrm{GF}}_s - Q_{s1} \quad (24)$$

and the heat balance at the GF is

$$Q^{(1)}_{\mathrm{GF}} = \tfrac{1}{3}\left(2\Delta H^0_{f\,\mathrm{CO}} - \Delta H^0_{f\,\mathrm{CO_2}}\right) + \tfrac{2}{3}\left(\Delta H^0_{f\,\mathrm{CO}} - \Delta H^0_{f\,\mathrm{H_2O}}\right) + N_{\mathrm{CO}}h^{\mathrm{GF}(2)}_{\mathrm{CO}} + N_{\mathrm{H_2}}h^{\mathrm{GF}(2)}_{\mathrm{H_2}} + h^{\mathrm{GF}(2)}_{\mathrm{CO_2}} \quad (25)$$

The sum of the first two terms in Eq. (25) is the heat Q_a absorbed in the reforming reactions. The last three terms are equal to the heat $Q^{(2)}_{\mathrm{GF}}$ at the GF exit, which was estimated under the conditions of 1700 K and 0.2 MPa. Equating $Q^{(2)}_{\mathrm{GF}}$ to the heat input to the SG1, we can write the heat balance at the SG1 as

$$Q^{(1)}_{\mathrm{SG1}} = Q_{s2} + Q^{\mathrm{GF}}_s + N_{\mathrm{CO}}h^{\mathrm{SG1}(2)}_{\mathrm{CO}} + N_{\mathrm{H_2}}h^{\mathrm{SG1}(2)}_{\mathrm{H_2}} + h^{\mathrm{SG1}(2)}_{\mathrm{CO_2}} \quad (26)$$

The last three terms in the right-hand side are the heat $Q^{(2)}_{\mathrm{SG1}}$ at the SG1 exit, which is assumed to be equal to the input heat $Q^{(1)}_{\mathrm{SG1_2}}$ to SG2 at 1100 K and 0.15 MPa. Q_{s2} is a part of the heat to the low-pressure ST. The heat balance at the HX/SG2 is

$$Q^{(1)}_{\mathrm{SG2}} = Q_{s3} + Q_{\mathrm{ph}} + N_{\mathrm{CO}}h^{\mathrm{SG2}(2)}_{\mathrm{CO}} + N_{\mathrm{H_2}}h^{\mathrm{SG2}(2)}_{\mathrm{H_2}} + N_{\mathrm{CO_2}}h^{\mathrm{SG2}(2)}_{\mathrm{CO_2}} \quad (27)$$

where the enthalpies at the exit are calculated at 355 K and 0.1 MPa. From Eqs. (24–27), we obtain the total heat input to the ST $Q_{s1} + Q_{s2} + Q_{s3} = Q_{\mathrm{ST}}$ as

$$Q_{\mathrm{ST}} = Q_{\mathrm{M}}(1-\eta_{\mathrm{M}}) - Q_a - Q_{\mathrm{ph}} - Q^{(2)}_{\mathrm{SG2}} \quad (28)$$

where $Q^{(2)}_{\mathrm{SG2}}$ is equal to the sum of the last three terms in Eq. (27). The work consumption at the syngas separator should be estimated under the same conditions as in other systems, that is,

$$W_{\mathrm{SGS}} = \left(N_{\mathrm{CO}} + N_{\mathrm{H_2}} + N_{\mathrm{CO_2}}\right)w_{\mathrm{SGS}} \quad (29)$$

For example, in the case of $\delta = 0.85$, W_{M}, W_{S}, and W_{D} are calculated to be 167.77×10^3, 104.76×10^3, and 9.68×10^3 kJ, respectively. The LOX work, the FC work, and those of the syngas separation and ST pumping are calculated to be 9.37×10^3, 16.55×10^3, 14.25×10^3, and 0.63×10^3 kJ, respectively. The total efficiency and the fraction of the dispersed power are $\eta = 61.32\%$ and $\varepsilon = 4.01\%$, respectively, for $\delta = 0.85$. In scenario 2, the hydrogen combustion heat is about 30% of the total syngas combustion heat, so that the dispersed power fraction exceeds 10% at first when δ becomes larger than 0.613.

D. System 4

It is assumed that the coal slag can be completely removed from the syngas and carbon dioxide mixture at the slag separator at 1700 K, so that an RFP can be used downstream of the GF. In this configuration, most of the heat from the GF can be transferred to the fuel and recycled to the MHD combustor. The fuel preheating temperature is assumed to be $T^{(2)}_{\mathrm{RFP}} = 1660$ K. It is assumed that the fuel of the mole number $N_{\mathrm{CO}} + N_{\mathrm{H_2}}\delta$ is pressurized adiabatically from the same inlet temperature and pressure as those in system 3 to the exit conditions as $p^{(2)}_{\mathrm{FC}} = 0.8$ MPa and $T^{(2)}_{\mathrm{FC}} = 643$ K. The compression work is calculated by Eq. (22) with enthalpies at the aforementioned temperatures and pressures. The heat Q_{ph} transferred to the fuel is calculated by Eq. (21) with the enthalpy values at the RFP inlet state $T^{(2)}_{\mathrm{FC}}$ and $p^{(2)}_{\mathrm{FC}}$ and those at the exit state $T^{(2)}_{\mathrm{RFP}}$ and $p^{(2)}_{\mathrm{RFP}} = 0.75$ MPa. The heat input to the MHD generator is also given by Eq. (23) with the preceding gaseous enthalpies evaluated at the preheater exit. We assume that the steam mole number injected into the GF is the same as in system 3 and also that the conditions at the syngas separator are the same. Therefore, the steam heat injected into the GF is determined by the heat balance at the fuel preheater and the SG, as follows:

$$Q_s = Q^{(2)}_{\mathrm{GF}} - Q_{\mathrm{ph}} - Q^{(2)}_{\mathrm{SG}} \quad (30)$$

where the heat at the SG exit is given by $Q^{(2)}_{\mathrm{SG}} = N_{\mathrm{CO}}h^{\mathrm{SG}(2)}_{\mathrm{CO}} + N_{\mathrm{H_2}}h^{\mathrm{SG}(2)}_{\mathrm{H_2}} + N_{\mathrm{CO_2}}h^{\mathrm{SG}(2)}_{\mathrm{CO_2}}$. In this system, the heat input to the GF should be kept constant even when the amount of the recycled hydrogen is changed. Therefore, the steam generation for the Rankine cycle should be performed at the MHD diffuser after the steam injection.

The regenerated heat can be calculated by the following relationship:

$$Q_{\mathrm{ST}} = Q_{\mathrm{M}}(1-\eta_{\mathrm{M}}) + Q^{\mathrm{GF}}_s - Q_a - Q^{(2)}_{\mathrm{GF}} \quad (31)$$

The numerical results for the case of $\delta = 0.85$ are as follows: W_M, W_{ST}, and W_D are 179.33×10^3, 199.15×10^3, and 9.68×10^3 kJ, respectively. The LOX work and the syngas separation work are the same as those in system 3. The FC work, the ST pump work and the steam injection work are 16.57×10^3, 1.37×10^3, and 0.84 kJ, respectively. Then, the total efficiency and the fraction of the dispersed power are 62.64% and 3.92%, respectively.

V. Results and Discussions

The efficiencies of systems 1–4 are presented in Fig. 9 with variation in the fractional power of the dispersed system from $\varepsilon = 0$ to 30%. It can be seen that the maximum efficiency can be obtained in each system at $\varepsilon = 0 (\delta = 1.0)$ and that the efficiency decreases with ε in each case. Although this tendency is due to the assumption of constant efficiency of the dispersed system, the assumption may be valid because the unit efficiency may not be dependent in principle on the total hydrogen use in the dispersed energy system, but the increase in the total work is mainly attributed to the increase in the number of units. The efficiency change with the fraction ε is largely dependent on the average efficiency of the dispersed system. If δ is lower than the assumed value, each system efficiency decreases more rapidly with ε from the value at $\varepsilon = 0$.

A comparison of the four systems shows that the highest efficiency is attainable in the MHD topping system with a recuperative fuel preheater. The difference between systems 4 and 3 is mainly attributed to the difference in the heat recycled from the fuel preheater to the topping unit. Even though the efficiency of system 3 is lower by $1.0 \sim 1.5\%$ than that of system 4, system 3 is worth noting because of its simplicity in the fuel preheater design and operation. Note in Fig. 9 that the effects of thermochemical pumping are clearly demonstrated in comparisons of scenarios 1 and 2 in the whole range of ε and also in comparisons of systems 1 and 2 in scenario 1 in the range $\varepsilon < 0.15$. We can say that the efficiency increase resulted from the thermochemical pumping is about $3 \sim 4\%$. The difference between systems 2 and 3 is mainly attributed to the difference in the heat of reaction and to the fuel preheating in system 3. The effect of thermochemical pumping in scenario 1 becomes small with increase in ε. This is because the GT exhaust heat in system 2 is regenerated in part by the gasification and by the steam generation at the SG, so that the effect of thermochemical pumping becomes small with decrease in δ. On the other hand, in system 1, the GT exhaust heat can be regenerated by the ST cycle with a constant fraction.

The efficiency characteristics shown in Fig. 9 were obtained without taking into account the work consumption for the liquefaction of the separated CO_2. If we assume the conventional compression method for liquefaction, the minimum work may be estimated by the enthalpy difference between the initial state of 355 K and 0.1 MPa and the liquid state assumed, for example, at 273 K and 5 MPa. If all of the separated CO_2 is assumed to be liquefied, the work consumption for 1-kmol CO_2 will be 15.68×10^3 kJ. The efficiencies of systems 2 and 4 with CO_2 liquefaction are plotted in Fig. 10. It can be seen that the efficiency drops are about 4% in both scenarios, whereas 60% is obtained in system 4 in the case of $\varepsilon = 0$.

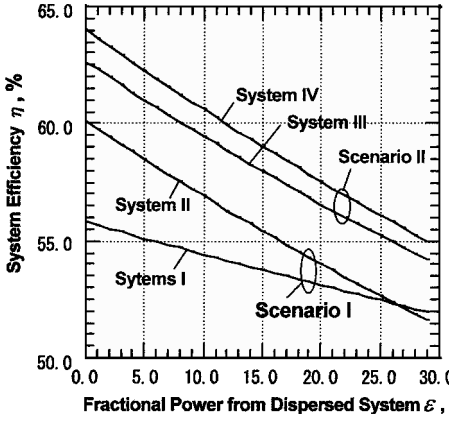

Fig. 9 Efficiencies of systems 1–4 and the dependence on the fractional power from the dispersed system: $\eta_{ST} = 48.5\%$, $\eta_M = 30\%$, and $\eta_D = 40\%$.

Table 1 Fractional work consumptions in systems 1–4 without CO_2 liquefaction

System	W_{total}, kJ	W_{LOX}	W_{SGS}	W_{FC}
1	24.24×10^3	0.4068	0.5175	——
2	26.21×10^3	0.3762	0.5582	——
3	42.40×10^3	0.2336	0.3377	0.4120
4	42.99×10^3	0.2294	0.3315	0.4045

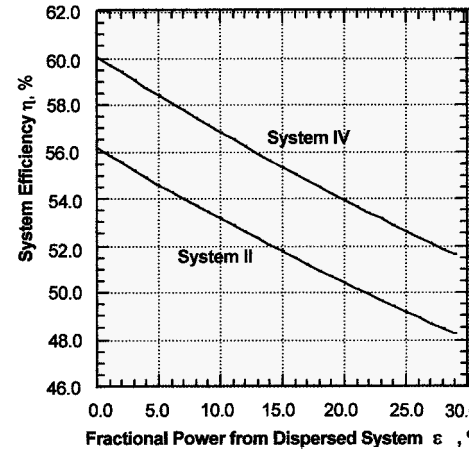

Fig. 10 Efficiencies of systems 2 and 4 with consideration of CO_2 liquefaction work estimated by enthalpy change from 355 K and 0.1 MPa to 273 K and 5 MPa.

The major electrical energy consumption in the present four model systems occurs in the LOX production and in the syngas separation processes in systems 1 and 2 plus the consumption in the fuel compressor in systems 3 and 4. The total work consumption and the fractions of each of W_{LOX}, W_{SGS}, and W_{FC} in systems 1–4 are given in Table 1. These results show that the developments of syngas and air separation technologies are key issues in the realization of the proposed scenarios. If the syngas separation pressure ratio assumed so far to be 5 could be reduced to 3, and the air separation could be performed with a membrane-type air separation method under a pressure ratio of, for example, 5, under isothermal compression, then the total efficiencies of systems 2–4 at $\delta = 1$ could be improved from those given in Fig. 9 up to 62.75, 65.28, and 66.67% respectively.

VI. Conclusions

The concept of CO_2-free fossil fuel power generation systems was proposed on the basis of a coupled configuration of central and local power generation systems. The role of the centralized large-scale station is to reform the carbonaceous fuel to hydrogen or hydrogen and carbon monoxide, to recover the carbon dioxide, and to distribute the hydrogen to the local dispersed-type power units. The reforming processes are either a relatively low-temperature carbon/steam reaction or high-temperature carbon/steam and carbon/carbon dioxide reactions. It was emphasized on the basis of the thermochemical pumping concept that the gasification heat and oxidants should be supplied from the exhaust of an appropriate topping unit driven by recycled syngas combustion products with pure oxygen. It was shown that the appropriate topping unit was a steam or water injection-type GT or a combustion-type MHD generator in the case of hydrogen/oxygen combustion, whereas in the case of hydrogen and carbon monoxide/oxygen combustion, only an MHD generator could be used for the topping unit because of the high temperature and enthalpy required for the exhaust gases.

The effect of thermochemical pumping and the effects of fuel preheating were evaluated in terms of total efficiencies and compared among the four models of combined systems under the assumptions of state-of-the-art unit performances. It was shown that the effect of thermochemical pumping amounts to a $3 \sim 4\%$ increase in total efficiency. The best performance was obtained in the case of an MHD topping with a recuperative-type fuel preheater combined with an ST system having an efficiency of from 64.0 to 55% when the fraction of the dispersed system power was varied from 0 to 29%. The efficiency of the GT topping system with thermochemical pumping was several percentage points lower than that of the MHD topping systems, but higher by several percent than that of the same GT topping system operated under the condition of conventional gasification schematics. Furthermore, it was shown that the total efficiency decreased with an increase in dispersed power. This is because the total power from the dispersed system is not determined by the unit power, but by the unit number. The effect of CO_2 liquefaction was estimated to be about a 4% decrease in total efficiency. The efficiency performances given in the present paper were estimated without consideration of any heat losses in system components for the purpose of comparison on a common basis. Therefore, the values given in this paper may certainly be overestimated, but have relative meaning. However, note that the efficiency of system 1 is almost the same order to or a few percentage points higher than that of the projected value of the IGCC ($\sim$5.5%).[12] Therefore, the presented results may be worth noting as target values of more realistic designs of systems 2–4.

The key technologies that must be developed to achieve the proposed scenarios are 1) an MHD generator driven by syngas/oxygen combustion plasmas, 2) a hydrogen/oxygen fired GT with low temperature or water injection, 3) carbon reforming processes with the exhaust heat and oxidants from the topping units, 4) efficient syngas and carbon dioxide separation, and 5) efficient oxygen production. However, note that none of these technologies are new, and all of these could certainly be achieved by further developments of the state-of-the-art technologies and by the restoration of the past MHD activities.

Acknowledgment

The author wishes to acknowledge the coal research staff of the Center for Advanced Research of Energy Technology at Hokkaido University for their valuable comments and discussions that contributed to this research effort.

References

[1]"IEA Statistics, Electricity Information 2000," International Energy Agency, Paris, 2000.

[2]Kayukawa, N., "Comparison of MHD Topping Combined Power Generation Systems," *Energy Conversion and Management*, Vol. 41, No. 18, 2000, pp. 1953–1974.

[3]Batenin, V. M., Zalkind, V. I., Kovbasyuk, V. I., Kretova, L. G., Rogov, B. V., and Schigel, S. S., "MHD Power Plants with Intracycle Thermochemical Regeneration in Power-Biotechnological Cycle," *Proceedings of the International Conference on MHD Power Generation and High Temperature Technology*, Vol. 1, 1999, pp. 232–252.

[4]Morison, G. F., "Coal-Fired MHD," IEA CR/06, April 1988, p. 24.

[5]Gannon, R. E., Stickler, D. B., and Kobayashi, H., "Coal Processing Employing Rapid Devolatilization Reactions in an MHD Power Cycle," Paper II. 2, April 1974.

[6]Fujii, S. (ed.), "JSME Mechanical Engineer's Handbook, B. Applications, B6: Power Plant Engineering," Japan Society of Mechanical Engineers, 1986, pp. B6–53.

[7]Tsukagoshi, K., Akita, E., and Nishida, M., "Development and Operating Experiences of the 502G, 1500°C Class Gas Turbine," *Journal of Gas Turbine Society of Japan*, Vol. 25, No. 100, 1998, pp. 2–7.

[8]Killirin, V. A., Sheindlin, A. E., Morozov, G. N., and Bryuskin, A. S., "The Present Status and Future Introduction to the Power Industry of Magnetohydrodynamic Plants," *Thermal Engineering*, Vol. 33, No. 10, 1986, pp. 59–67.

[9]Yoshikawa, K., "High Efficiency Energy Extraction from Coal/Waste Using High Temperature Air," *Proceedings of the International Conference on MHD Power Generation and High Temperature Technology*, Vol. 2, 1999, pp. 603–607.

[10]Uchida, H. (ed.), "Thermophysical Properties of Fluids," *JSME Data Book*, Japan Society of Mechanical Engineers, 5th ed., 1994.

[11]Chase, Jr., M. W., Davies, J. R., Downey, Jr., J. R., Frurip, D. J., McDonald, R. A., and Syverud, A. N., "JANAF Thermochemical Tables," *Journal of Physical and Chemical Reference Data*, Supplement, Vol. 14, 3rd ed., 1985.